A Novel Flexure Parallel Micromanipulator Based on Multi-Level Displacement Amplifier

Dan Zhang[1,2] *, Zhen Gao[1], Matteo Malosio [3], Gianmarc Coppola[1]
[1] Faculty of Engineering and Applied Science, University of Ontario Institute of Technology
Oshawa, ON, Canada, L1H 7K4
[2] Qingdao Technological University, Qingdao, Shandong, China
[3] Institute of Industrial Technologies and Automation, National Research Council
Bassini 15, 20133 Milano, Italy
*Corresponding author, Email: Dan.Zhang@uoit.ca

***Abstract*-The conventional flexure parallel micromanipulators (FPM) usually suffer from small stroke. The performances of a FPM are highly related with the stroke of each actuated limb and the constraints including the non-actuated limbs. To conquer the drawbacks of the small workspace of the conventional FPM, the mechanism for displacement amplification would make a great contribution when it is imported into the design of the actuated limbs. This research is focused on a unique FPM based on multi-level displacement amplifier. Firstly, the structure modeling based on compact modular design is introduced. The macro/micro analysis of the displacement amplifier is conducted. Then, the comprehensive finite-element modeling including the strain and total deformation are implemented to examine the actual mechanical behavior of the proposed mechanism. The developed method and technology provide a promising solution to enhance the performance of the generic FPMs.**

Keywords-Flexure parallel micromanipulator; multi-level displacement amplifier; finite-element analysis; symmetrical topology structure

I. INTRODUCTION

With the rapid and extensive development in both theories and applications in the past several decades, parallel manipulator has become a nondisplaceable technology which reflect its merits in areas of machine tools [1-6], sensors and transducers [7-10], micro devices and MEMS systems [11-15], and motion platforms [16-18], majorly due to its distinct advantages including higher positioning precision, higher dynamic performance, higher stiffness, less accumulative error and easier for inverse kinematic modeling.

In the area of multi-axis micro-positioning, many scholars have developed different types of flexure parallel micromanipulators to achieve the expected goals [19-25]. In [20], a 3-limb 6-DOF parallel micromanipulator with 3PPSP structure was investigated. In each limb, there are two actuator joints which are integrated in a x-y plane attached to the base. In [21], the special materials including olyvinylidene fluoride and lead zirconium titanate were utilized to develop the piezoelectric actuators for the vibration control of a planar compliant parallel manipulator. In [22], a nanopositioning parallel stage which has high bandwidth, high motion range and low cross-coupling was developed so that control strategies based on single-input single-output for trajectory tracking was available. In [23], a compliant positioned based on parallel kinematic structure was dually driven by six piezoelectric actuators and six piezoelectric ceramics. Through testing, it could be found that this structure simultaneously generated wide motion range and high precision. In [24], the pseudo rigid-body model was calculated for a 3-DOF flexure parallel micromanipulator in which three limbs are perpendicular to each other. In [25], the electromagnetic actuators with less than 0.1% full-scale position error were fabricated to drive a six-axis compliant parallel mechanism.

However, since every coin has its opposite side, especially for the case of parallel micromanipulators, the natural limitation of the small stroke of the traditional actuators restrict the workspace and the limb displacement in a small region. Regarding this, a unique FPM with 3-DOF based on multi-level displacement amplifier is designed for the potential application situations where large motion range is required in a micro- or nano- positioning environment. The proposed multi-level displacement amplifier based on a series of flexure hinges is integrated in each compliant limb as a monolithic structure which is driven by piezoelectric actuator.

The rest part of this paper is organized as follows: the conceptual designs and the kinematics modeling of the displacement amplifier and related planar/spatial flexure parallel micromanipulators are introduced Sections 2 and 3. In Section 4, the finite-element analysis is conducted to examine the static performance of the proposed FPM. Final section gives the conclusion.

II. CONCEPTUAL DESIGN

As the key part of the flexure parallel micromanipulators, the conceptual structure of the multi-level displacement

 ISBN: 978-1-61208-208-0

amplifier is illustrated in Fig. 1. The piezoelectric actuator will be placed in the middle of the mechanism between the two convex stages connected to the inner bars. The four free lower/upper ends are attached to a fixed base. Through multi-stage amplification of the original displacement, large workspace of the end-effector can be achieved.

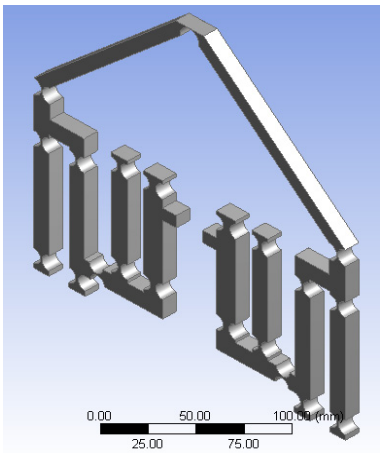

Figure 1. The CAD model of the proposed displacement amplifier

The following figure shows how to combine two multi-level displacement amplifiers to develop a high-precision XY positioning stage.

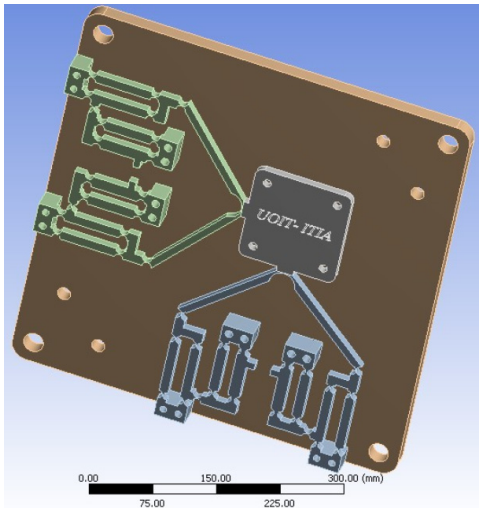

Figure 2. Planar flexure parallel micromanipulator based on displacement amplifier

Figure 3 displays a spatial FPM with large motion range for the potential application in micro positioning environment. The mechanism is utilized as the case study in this research to verify its characteristics.

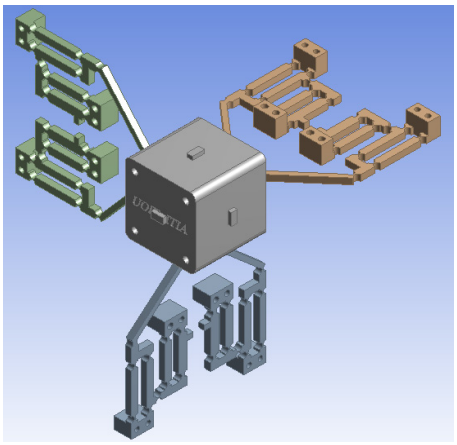

Figure 3. Spatial flexure parallel micromanipulator based on displacement amplifier

III. ANALYSIS OF THE DISPLACEMENT AMPLIFIER

A. Macro Analysis

In this subsection, it is focused on the amplification analysis of the proposed displacement amplifier based on the macro dimensions which are shown in Fig. 4.

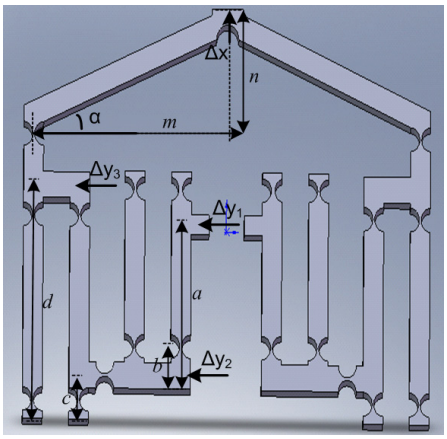

Figure 4. The macro dimensions of the proposed displacement amplifier

When the deformation Δy_1 occurs, it has

$$\Delta y_2 = \frac{b}{a}\Delta y_1 \tag{1}$$

$$\Delta y_3 = \frac{d}{c}\Delta y_2 \tag{2}$$

Then, the output displacement can be derived as,

$$\begin{aligned}\Delta x &= n - \sqrt{m^2 + n^2 - (m + \Delta y_3)^2} \\ &= n - \sqrt{n^2 - 2m \cdot \frac{b}{a} \cdot \frac{d}{c} \cdot \Delta y_1 - (\frac{b}{a} \cdot \frac{d}{c} \cdot \Delta y_1)^2}\end{aligned} \tag{3}$$

Thus, the amplification k is given as,

$$k = \frac{\Delta x}{\Delta y_1} = \frac{n - \sqrt{n^2 - 2m \cdot \frac{b}{a} \cdot \frac{d}{c} \cdot \Delta y_1 - (\frac{b}{a} \cdot \frac{d}{c} \cdot \Delta y_1)^2}}{\Delta y_1} \quad (4)$$

B. Micro Analysis

The circular flexure hinge can be expressed with the following compliance matrix,

$$\boldsymbol{C}_c = \begin{bmatrix} c_x^{F_x} & 0 & 0 & 0 & 0 & 0 \\ 0 & c_y^{F_y} & 0 & 0 & 0 & c_y^{M_z} \\ 0 & 0 & c_z^{F_z} & 0 & c_z^{M_y} & 0 \\ 0 & 0 & 0 & c_{\theta_x}^{M_x} & 0 & 0 \\ 0 & 0 & c_{\theta_y}^{F_z} & 0 & c_{\theta_y}^{M_y} & 0 \\ 0 & c_{\theta_z}^{F_y} & 0 & 0 & 0 & c_{\theta_z}^{M_z} \end{bmatrix} \quad (5)$$

As the most important element, $c_{\theta_z}^{M_z}$ is written as,

$$c_{\theta_z}^{M_z} = \frac{\theta_z}{M_z} = \frac{24R}{Ebt^3(2R+t)(4R+t)^3}[t(4R+t)(6R^2+4Rt+t^2) + 6R(2R+t)^2\sqrt{t(4R+t)}\tan^{-1}\sqrt{1+\frac{4R}{t}}] \quad (6)$$

where, R denotes the radius of circular arc. E is the elastic modulus of selected material. b represents the width of the hinge. t is the thickness of the thinnest part of the circular flexure hinge.

The elastic potential energy of the half part of a single displacement amplifier can be derived as,

$$E_e = \sum_{i=1}^{9} \frac{1}{2c_{\theta_z}^{M_z}} \theta_{zi}^2 \quad (7)$$

The above equation can be rewritten as,

$$E_e = \sum_{i=1}^{9} \frac{1}{48R} \cdot \frac{Ebt^3\theta_{zi}^2(2R+t)(4R+t)^3}{[t(4R+t)(6R^2+4Rt+t^2)+6R(2R+t)^2\sqrt{t(4R+t)}\tan^{-1}\sqrt{1+\frac{4R}{t}}]} \quad (8)$$

IV. FINITE ELEMENT ANALYSIS

Finite element analysis (FEA) is a paramount method to test the performance of the flexure based compliant parallel manipulator. The different selection of materials also affects the practical characteristics. With a critical evaluation of design criteria based on various materials, stainless steel is chosen whose properties is described in Table 1.

TABLE I. MATERIAL PROPERTIES

Density	7.85e-006 kg mm^{-3}
Coefficient of Thermal Expansion	1.2e-005 C^{-1}
Specific Heat	4.34e+005 mJ kg^{-1} C^{-1}
Thermal Conductivity	6.05e-002 W mm^{-1} C^{-1}
Resistivity	1.7e-004 ohm mm

Figure 5 illustrates the strain and deformation results under external forces applied on one displacement amplifier. When $F = 1N$, the maximal/minimal equivalent elastic strain is 2.8858×10^{-7} *mm*/*mm* and 0 respectively, and the maximal total deformation is 3.198×10^{-5} *mm*. When $F = 6N$, the maximal/minimal equivalent elastic strain is 1.7351×10^{-6} *mm*/*mm* and 4.4355×10^{-20} *mm*/*mm* respectively, and the maximal total deformation is 1.9188×10^{-4} *mm*. When $F = 11N$, the maximal/minimal equivalent elastic strain is 3.1744×10^{-6} *mm*/*mm* and 8.1323×10^{-20} *mm*/*mm* respectively, and the maximal total deformation is 3.5178×10^{-4} *mm*. When $F = 16N$, the maximal/minimal equivalent elastic strain is 4.6173×10^{-6} *mm*/*mm* and 1.1828×10^{-19} *mm*/*mm* respectively, and the maximal total deformation is 5.1168×10^{-4} *mm*. When $F = 21N$, the maximal/minimal equivalent elastic strain is 6.0601×10^{-6} *mm*/*mm* and 1.5524×10^{-19} *mm*/*mm* respectively, and the maximal total deformation is 6.7158×10^{-4} *mm*.

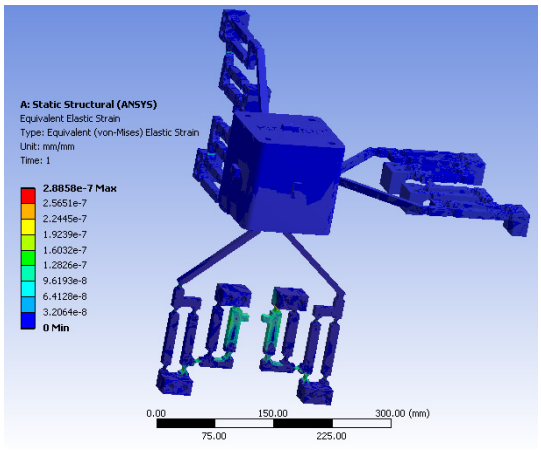

(a)

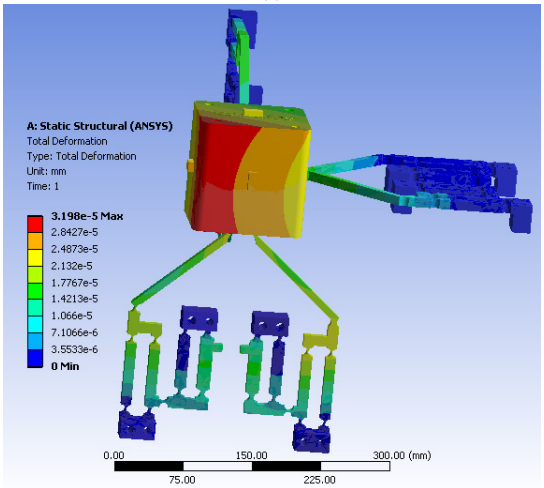

(b)

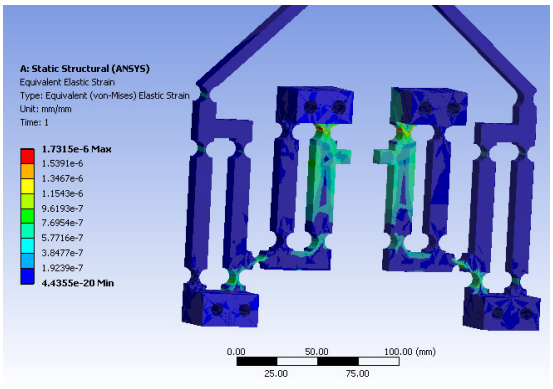
A: Static Structural (ANSYS)
Equivalent Elastic Strain
Type: Equivalent (von-Mises) Elastic Strain
Unit: mm/mm
Time: 1
1.7315e-6 Max
1.5391e-6
1.3467e-6
1.1543e-6
9.6193e-7
7.6954e-7
5.7716e-7
3.8477e-7
1.9239e-7
4.4355e-20 Min
0.00 50.00 100.00 (mm)
25.00 75.00

(c)

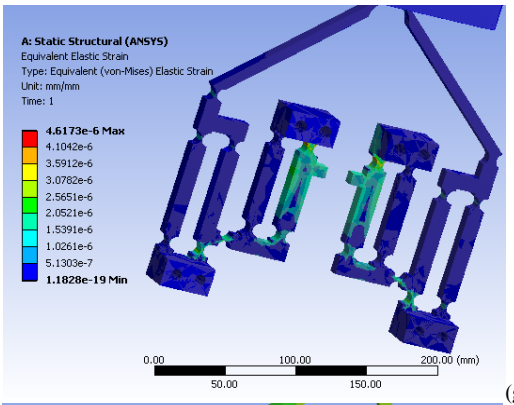
A: Static Structural (ANSYS)
Equivalent Elastic Strain
Type: Equivalent (von-Mises) Elastic Strain
Unit: mm/mm
Time: 1
4.6173e-6 Max
4.1042e-6
3.5912e-6
3.0782e-6
2.5651e-6
2.0521e-6
1.5391e-6
1.0261e-6
5.1303e-7
1.1828e-19 Min
0.00 100.00 200.00 (mm)
50.00 150.00

(g)

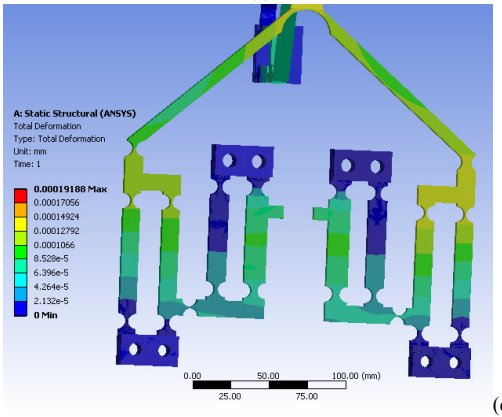
A: Static Structural (ANSYS)
Total Deformation
Type: Total Deformation
Unit: mm
Time: 1
0.00019188 Max
0.00017056
0.00014924
0.00012792
0.0001066
8.528e-5
6.396e-5
4.264e-5
2.132e-5
0 Min
0.00 50.00 100.00 (mm)
25.00 75.00

(d)

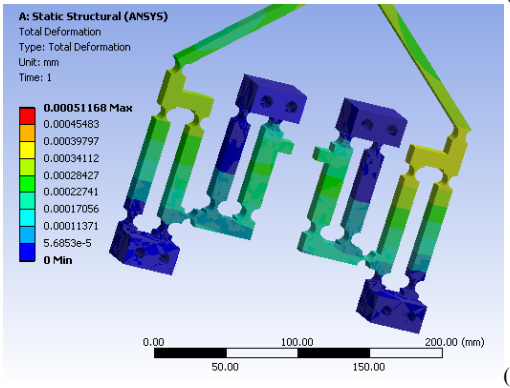
A: Static Structural (ANSYS)
Total Deformation
Type: Total Deformation
Unit: mm
Time: 1
0.00051168 Max
0.00045483
0.00039797
0.00034112
0.00028427
0.00022741
0.00017056
0.00011371
5.6853e-5
0 Min
0.00 100.00 200.00 (mm)
50.00 150.00

(h)

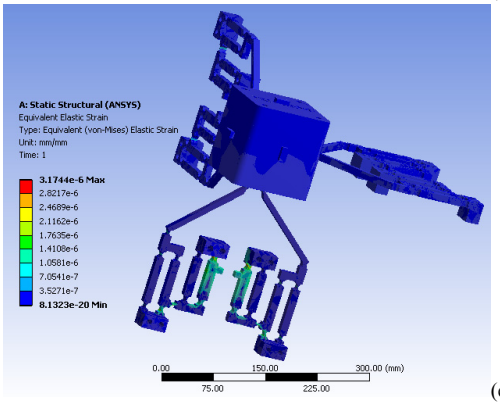
A: Static Structural (ANSYS)
Equivalent Elastic Strain
Type: Equivalent (von-Mises) Elastic Strain
Unit: mm/mm
Time: 1
3.1744e-6 Max
2.8217e-6
2.4689e-6
2.1162e-6
1.7635e-6
1.4108e-6
1.0581e-6
7.0541e-7
3.5271e-7
8.1323e-20 Min
0.00 150.00 300.00 (mm)
75.00 225.00

(e)

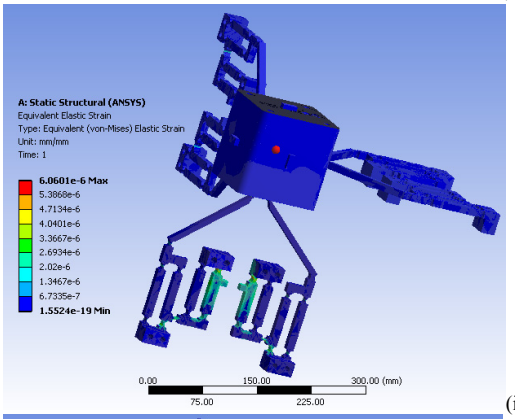
A: Static Structural (ANSYS)
Equivalent Elastic Strain
Type: Equivalent (von-Mises) Elastic Strain
Unit: mm/mm
Time: 1
6.0601e-6 Max
5.3868e-6
4.7134e-6
4.0401e-6
3.3667e-6
2.6934e-6
2.02e-6
1.3467e-6
6.7335e-7
1.5524e-19 Min
0.00 150.00 300.00 (mm)
75.00 225.00

(i)

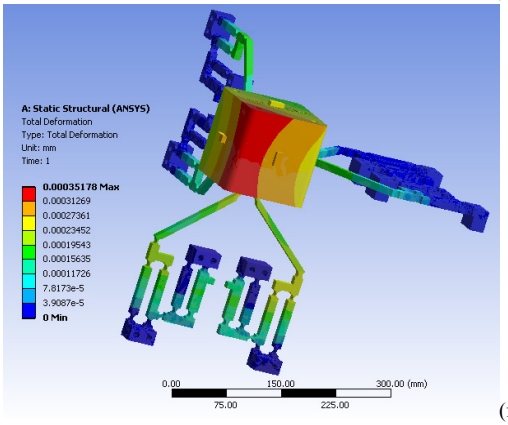
A: Static Structural (ANSYS)
Total Deformation
Type: Total Deformation
Unit: mm
Time: 1
0.00035178 Max
0.00031269
0.00027361
0.00023452
0.00019543
0.00015635
0.00011726
7.8173e-5
3.9087e-5
0 Min
0.00 150.00 300.00 (mm)
75.00 225.00

(f)

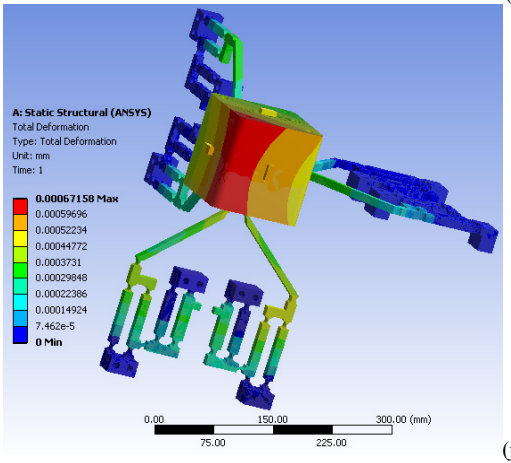
A: Static Structural (ANSYS)
Total Deformation
Type: Total Deformation
Unit: mm
Time: 1
0.00067158 Max
0.00059696
0.00052234
0.00044772
0.0003731
0.00029848
0.00022386
0.00014924
7.462e-5
0 Min
0.00 150.00 300.00 (mm)
75.00 225.00

(j)

Figure 5. The strain and deformation results under external forces applied on one displacement amplifier

Figure 6 (a) shows the fitting curve of the maximal total deformation under different external forces. Figure 6 (b) and (c) describes the fitting curve of the maximal/minimal equivalent elastic strain under different external forces respectively. It can be found that the proposed FPM based on displacement amplifier has advantageous characteristics in terms of linearity and sensitivity.

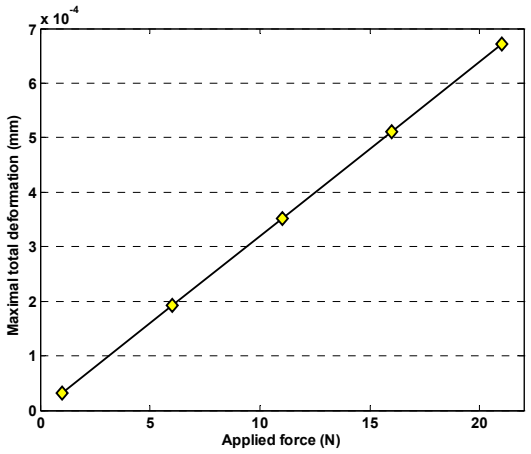

(a)

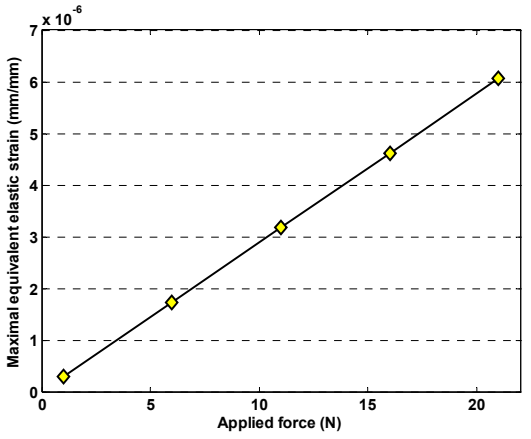

(b)

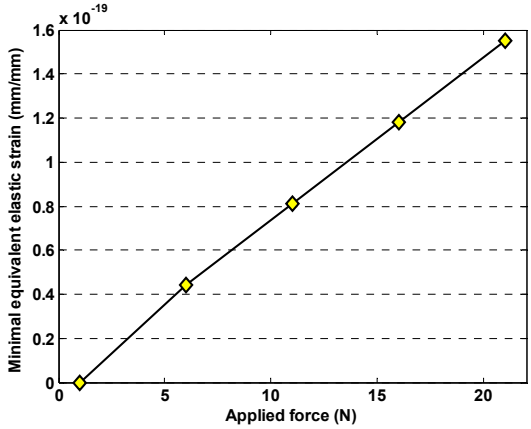

(c)

Figure 6. The fitting curve of the deformation and strain

The resonant frequency of FPM can be utilized for its modal analysis. The classic sample of a mechanical resonance is a discrete system consisting of a mass attached to a spring with a constant force. The proposed FPM based on displacement amplifier is more complicated than a simple spring, which implies that it may contain more than one resonance frequency. Through simulation, it can be found in Fig. 7 that there are at least four resonance frequencies. The total deformation under different frequency inputs are depicted in Fig. 8.

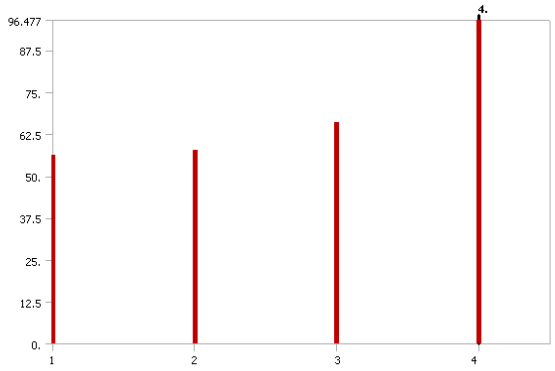

Figure 7. Mode and resonance frequency

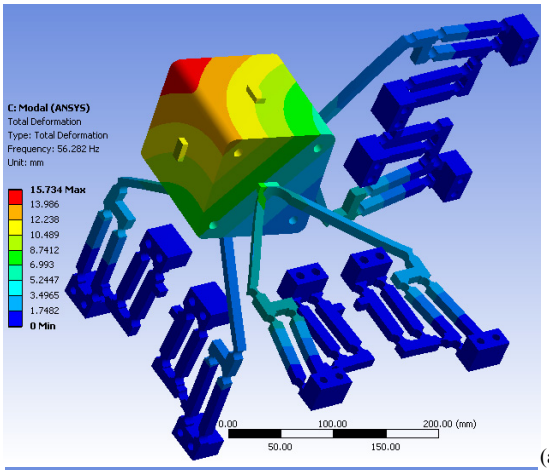

(a)

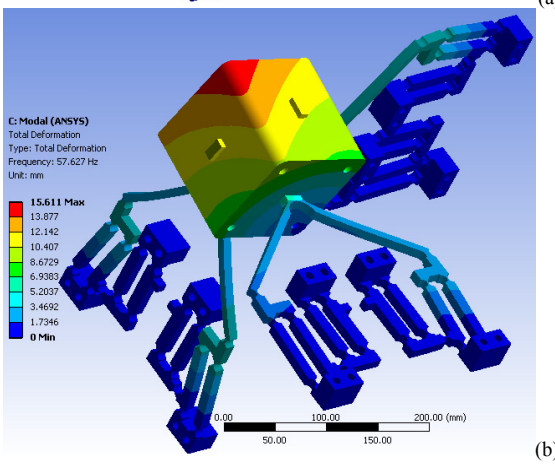

(b)

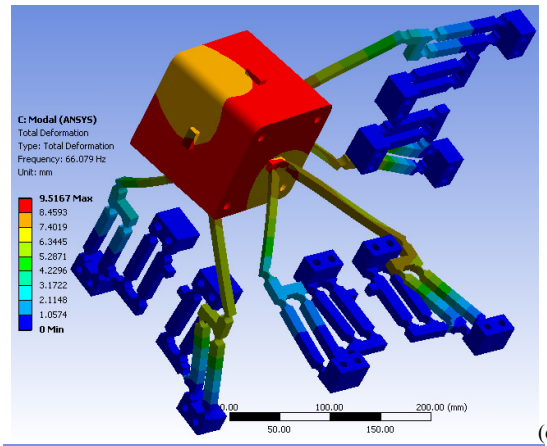

(c)

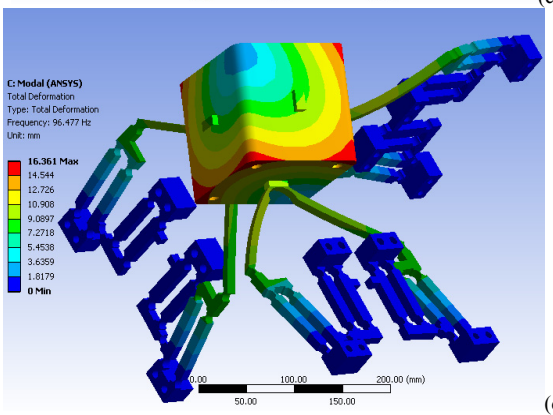

(d)

Figure 8. Modal analysis of the total deformation under different frequency conditions; (1) the first modal with the resonance frequency 56.282Hz, (2) the second modal with the resonance frequency 57.627Hz, (3) the third modal with the resonance frequency 66.079Hz, (4) the fourth modal with the resonance frequency 96.477Hz.

To analysis the forced vibrations and the steady-state response, harmonic response can be analyzed when the following assumptions are given: static structural modeling is implemented firstly and damping is neglected for modal analysis. Figure 9 reflects the frequency response of the directional deformation in z-axis, normal elastic strain and directional acceleration in z-axis. An external force of 10N is applied on the moving platform in z-direction.

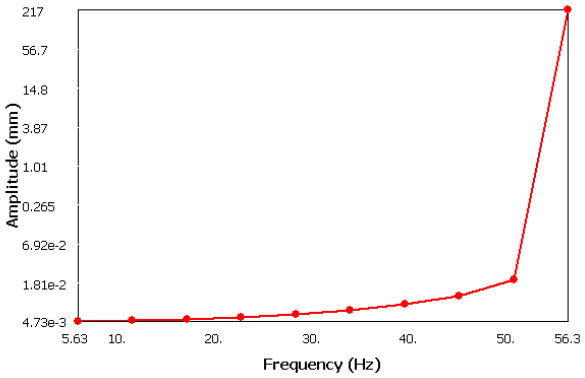

(a)

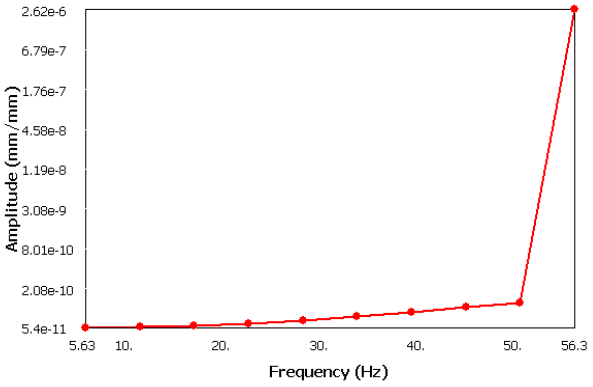

(b)

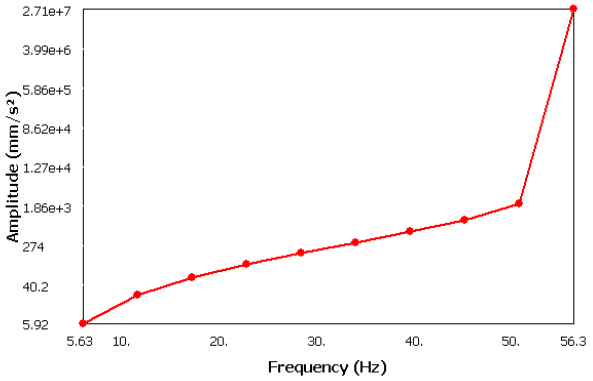

(c)

Figure 9. Frequency response when an external force of 10N is applied on the moving platform in z-direction when the first level mode 56.282 Hz is attached; a) directional deformation, b) normal elastic strain, c) directional acceleration

V. CONCLUSIONS AND FUTURE WORK

This research investigates on the conceptual design and performance analysis of a novel multi-level displacement amplifier based flexure parallel micromanipulator in which the stroke direction is perpendicular to the translation of the end-effector. The displacement amplifier is analyzed in macro and micro aspects. The finite element analysis proves the feasibility of the proposed design and it can be found that the proposed FPM has advantageous characteristics including high compliance, high linearity and high sensitivity. The proposed models and methods provide a new viewpoint for the development of compliant parallel micromanipulators. To eliminate the bending in undesired points, the improved symmetrical topology structures both in plane and in space will be developed for the future study. A physical prototype will be fabricated and tested. The experiments will be conducted to deeply explore the actual performances of the proposed design.

 ISBN: 978-1-61208-208-0

ACKNOWLEDGEMENTS

The authors would like to thank the financial support from the Natural Sciences and Engineering Research Council of Canada (NSERC). The authors gratefully acknowledge the financial support from Canada Research Chairs program, Early Researcher Award from Ministry of Research and Innovation of Ontario and the MITACS-NCE Research Project.

REFERENCES

[1] D.A. Axinte, J.M. Allen, R. Anderson, I. Dane, L. Uriarte, and A. Olara, " Free-leg Hexapod: A novel approach of using parallel kinematic platforms for developing miniature machine tools for special purpose operations," CIRP Annals - Manufacturing Technology, Volume 60, Issue 1, 2011, pp. 395-398

[2] H. Chanal, E. Duc, J.Y. Hascoët, and P. Ray, "Reduction of a parallel kinematics machine tool inverse kinematics model with regard to machining behavior," Mechanism and Machine Theory, Volume 44, Issue 7, July 2009, pp. 1371-1385

[3] D. Zhang, Z. Bi, and B. Li, "Design and kinetostatic analysis of a new parallel manipulator," Robotics and Computer-Integrated Manufacturing, Vol. 25, pp. 782-791, 2009.

[4] X. Ren, Z. Feng, and C. Su, "A new calibration method for parallel kinematics machine tools using orientation constraint," International Journal of Machine Tools and Manufacture, Volume 49, Issue 9, July 2009, pp. 708-721

[5] Y. Li, J. Wang, X. Liu, and L. Wang, "Dynamic performance comparison and counterweight optimization of two 3-DOF parallel manipulators for a new hybrid machine tool," Mechanism and Machine Theory, Volume 45, Issue 11, November 2010, pp. 1668-1680

[6] G. Gao, Y. Zhang, and L. Xue, "Sliding Mode Control with a Disturbance Observer for a Virtual Axis Machine Tool Parallel Mechanism," Energy Procedia, Vol. 13, 2011, Pages 610-616

[7] R. Ranganath, P. S. Nair, T. S. Mruthyunjaya, and A. Ghosal, "A force-torque sensor based on a Stewart platform in a near-singular configuration," Mechanism and Machine Theory, Vol. 39, No. 9, pp. 971-998, 2004.

[8] Z. L. Jin, F. Gao, and X. H. Zhang, "Design and analysis of a novel isotropic six-component force/torque sensor, Sensors and Actuators A: Physical, Vol. 109, pp. 17-20, 2003.

[9] G. S. Kima, H. J. Shina, and J. W. Yoon, "Development of 6-axis force/moment sensor for a humanoid robot's intelligent foot," Sensors and Actuators A: Physical, Vol, 141, No. 2, pp. 276-281, 2008

[10] Y. L. Hou, D. X. Zeng, J. T. Yao, K. J. Kang, L. Lu, and Y. S. Zhao, "Optimal design of a hyperstatic Stewart platform-based force/torque sensor with genetic algorithms," Mechatronics, Vol. 19, pp. 199-204, 2009

[11] Y. Yue, F. Gao, X. Zhao, and Q. Ge, "Relationship among input-force, payload, stiffness and displacement of a 3-DOF perpendicular parallel micro-manipulator," Mechanism and Machine Theory, Volume 45, Issue 5, 2010, pp. 756-771

[12] Tung-Li Wu, Jia-Hao Chen, and Shuo-Hung Chang, A Six-DOF Prismatic-Spherical-Spherical Parallel Compliant Nanopositioner, IEEE Transactions on Ultrasonics, Ferroelectrics, and Frequency Control, vol. 55, no. 12, December 2008, pp. 2544-2551

[13] D.S. Kang, T.W. Seo, Y.H. Yoon, B.S. Shin, X-J Liu, and J. Kim, "A Micro-positioning Parallel Mechanism Platform with 100-degree Tilting Capability," CIRP Annals - Manufacturing Technology, Volume 55, Issue 1, 2006, pp. 377-380

[14] K. A. Jensen, C. P. Lusk, and L. L. Howell, "An XYZ micromanipulator with three translational degrees of freedom," Robotica, Vol. 24, No. 3, pp. 305-314, 2006.

[15] J. Palmer, B. Dessent, J. F. Mulling, T. Usher, E. Grant, J. W. Eischen, A. Kingon, and P. Franzon, "The design and characterization of a novel piezoelectric transducer-based linear motor," IEEE/ASME Transaction on Mechatronics, Vol. 13, pp. 441-450, 2004

[16] R. Franci, V. Parenti-Castelli, C. Belvedere, and A. Leardini, "A new one-DOF fully parallel mechanism for modelling passive motion at the human tibiotalar joint," Journal of Biomechanics, Volume 42, Issue 10, 22 July 2009, pp. 1403-1408

[17] E. Ottaviano, M. Ceccarelli, and G. Castelli, "Experimental results of a 3-DOF parallel manipulator as an earthquake motion simulator," ASME Conf. Proc. IDETC/CIE, 2004.

[18] R. Kelaiaia, O. Company, and A. Zaatri, "Multiobjective optimization of a linear Delta parallel robot," Mechanism and Machine Theory, Volume 50, April 2012, pp. 159-178

[19] F. Mert Sasoglu, Andrew J. Bohl, Kathleen B. Allen, and Bradley E. Layton, "Parallel force measurement with a polymeric microbeam array using an optical microscope and micromanipulator," Computer Methods and Programs in Biomedicine, Volume 93, Issue 1, January 2009, pp. 1-8

[20] L. Wang, W. Rong, M. Feng, T. Liu, and L. Sun, "Calibration of a 6-DOF parallel micromanipulator for nanomanipulation," 2010 3rd International Nanoelectronics Conference, pp.38- 139

[21] Bongsoo Kang and James K. Mills, "Study on Piezoelectric Actuators in Vibration Control of a Planar Parallel Manipulator," Proceedings of the 2003 IEEE/ASME International Conference on Advanced Intelligent Mechatronics (AIM 2003), pp. 1268-1273

[22] Y. K. Yong, S. Aphale and S. O. R. Moheimani, "Design, identification and control of a flexure-based XY stage for fast nanoscale positioning," IEEE Trans. Nanotechnology, vol. 8, no. 1, pp. 46-54, 2009.

[23] W. Dong, L. N. Sun, and Z. J. Du, "Design of a precision compliant parallel positioned driven by dual piezoelectric actuators," Sensors and Actuators A 135 (2007) pp. 250-256

[24] X. Tang, H.-H. Pham, Q. Li, and I.-M. Chen, "Dynamic analysis of a 3-DOF flexure parallel micromanipulator," in Proc. IEEE Conf. on Robotics, Automation and Mechatronics, pp. 95-100, 2004.

[25] M. Culpepper and G. Anderson, "Design of a low-cost nano manipulator which utilizes a monolithic, spatial compliant mechanism," Precision Engineering 28 (2004) pp. 469-482

 ISBN: 978-1-61208-208-0